Description of the fluorescence intensity time trace of collections of CdSe nanocrystal quantum dots based on single quantum dot fluorescence blinking statistics

Inhee Chung, James B. Witkoskie, Jianshu Cao, and Moungi G. Bawendi
Department of Chemistry and Center for Materials Science, Massachusetts Institute of Technology, 77 Massachusetts Avenue, Cambridge, Massachusetts 02139, USA
(Received 28 June 2005; published 20 January 2006)

This paper analyzes the observed phenomenology of the fluorescence time trace of collections of quantum dots (QDs) in terms of the model parameters that characterize the fluorescence blinking statistics of single QDs. We demonstrate that the non-universal dynamics that appear in fluorescence time traces of collections of QDs at short time scales are related to the universal dynamics that appear at longer time scales. We explore how the extent of time separation between the short and long dynamics affects the transition region and the dynamics at longer time scales. We suggest a methodology to extract single QD statistical model parameters from experimental fluorescence time traces of collections of QDs. We explore theoretical time traces and their experimental analogs for three different cases that span the diverse nonuniversal dynamics that appear at short time scales.

DOI: 10.1103/PhysRevE.73.011106 PACS number(s): 05.40.−a, 78.67.Bf, 78.55.−m, 82.37.−j

I. INTRODUCTION

Semiconductor nanocrystals, also known as quantum dots (QDs), have potential in a wide range of applications due to their unique optical properties. These properties include a higher photochemical stability than most organic emitters and a spectrally broad absorption window coupled to a narrow emission band that is tunable with the size of the QD. QDs can be incorporated into optical gain media with a high volume fraction [1–5] and into optoelectronic devices, such as light emitting devices (LED) [6–10]. Single quantum dot fluorescence has also been used in biological imaging studies [11–15].

One of the most intriguing photo-physical properties of single QDs is the intermittency [16,17] observed in their fluorescence under continuous laser excitation [18–20]. This fluorescence intermittency has generally been described using power-law statistics [7,18–27], although recently different statistics for the intermittency were reported when QDs were placed in the presence of β-mercaptoethanol (BME) [28]. We have previously shown that the fluorescence intermittency in single CdSe QDs becomes ergodic in the long time limit, and that as a consequence the fluorescence time trace of collections of large numbers of QDs exhibits a photo-decay to a final steady state [29]. This decrease in fluorescence intensity to a steady state appears to be a universal phenomenon observed in collections of QDs (CQDs). The onset of the decay and the steady state amplitude, however, vary greatly with different types of QDs and with the specific experimental conditions. Before this characteristic decay, fluorescence time traces of a CQD can exhibit a wide variety of dynamics, including an initial decay, an initial brightening, or a brightening that follows an initial decay. All of these early dynamics vary greatly in duration and extent depending on the type of QDs and other experimental conditions such as excitation intensity and temperature. At the single QD level, however, approximate power-law statistics are obtained for the on and off-times for a wide time window. These observations beg the following question: Can the early dynamics of CQDs be explained consistently with the later universal dynamics, using the observed blinking statistics of single QDs? Previously, photodecay and photobrightening effects have been individually reported in various papers [30,31], but there has not yet been an attempt to address both phenomena coherently within a single quantitative model. In this paper, by constructing complete fluorescence time traces of CQDs starting from the blinking statistics of single QDs, we show how the early non-universal dynamics are connected to the later universal dynamics. We also suggest a methodology to extract parameters of the blinking statistics of single QDs from the fluorescence time trace of a CQD.

Fluorescence blinking in single CdSe QDs can be characterized by a two-state flipping process determined by two waiting times: the "on time," during which the QD fluoresces (bright state), and the "off time," during which no emission from the QD is detected within the experimental noise (dark state). Experiments have shown that the two-state flipping process is an adequate description of the system within the observed time ranges because no correlations between flipping events are observed. Any deviations from this description occur on timescales that are much shorter than those of interest. Although the microscopic mechanism responsible for the blinking phenomenon has not yet been understood, the dark state has been associated with a charged QD, where a fast nonradiative Auger mechanism [16,32,33] effectively quenches the emission [34]. We have previously described the fluorescence blinking statistics of single QDs using bounded power-law statistics for the on- and off-waiting times [29]. Using these bounded power-law statistics, the universal decay dynamics of CQDs in the long-time limit was successfully described by a probability function $f_{on}(t)$, where $f_{on}(t)$ is the probability to find a QD in a bright state (i.e., to be "on") at time t. In our previous work, we assumed that the lower bounds for the on and off-time power laws were light induced and identical. It is the mismatch between

the upper bounds for the on and off-times (smaller bound for on compared to off) that leads to the characteristic decay to a steady state observed in collections of QDs. The decay begins when the upper bound for the on time is reached, and settles to a steady state approximately when the upper bound for the off times is reached. We have previously shown that these upper bounds can be extracted from the long time fluorescence trace of a CQD [29]. In experiments where the bin-size is large compared to the lower bounds, the time trace of the fluorescence from a CQD generally exhibits three time windows: (1) an initial transient equilibrium state followed by (2) a photo decay, and finally (3) a steady state. The photo decay and the steady state are referred to as the long-time dynamics in this paper. If the bin size is comparable to the lower bounds, however, nonuniversal features are often briefly observed prior to the transient equilibrium state. We refer to these features as the short-time dynamics. Our previous work omitted a description of the short-time dynamics [29]. The transient equilibrium state corresponds to a transition region between the short- and long-time dynamics.

In the present paper, we rigorously investigate the effect of the time separation between the short- and long-time dynamics on $f_{\mathrm{on}}(t)$, especially with respect to the values of the transient equilibrium and steady states. We provide equations for the values of the transient equilibrium and steady states that are valid in the limit of large time separation. We show that asymmetric lower bounds can (1) explain the nonuniversal short-time dynamics before the transient equilibrium state and (2) quantitatively affect the details of the transient equilibrium state and long-time dynamics where universal characteristics remain intact. In the following background section, we describe the modified probability density functions for on- and off-times that are used to facilitate numerical calculation of $f_{\mathrm{on}}(t)$, and we provide an overview of the paper.

II. BACKGROUND

We use probability density functions for on and off times that are similar to those used in our previous work [29]. The blinking of QDs is assumed to follow an alternating renewal process, where on- and off-waiting times are distributed as power laws with exponents that are $\sim(-0.5)$. Long-time exponential cutoffs to the power-law distributions give upper limits to the duration of on times as experimentally observed at the single QD level, and of off-times, as deduced from the observed fluorescence time traces of CQDs [29]. Normalizability of the distributions implies the existence of lower cutoffs. In our previous work we assumed abrupt lower cutoffs with values given by the average time between optical excitations [29]. In this work, we use arbitrary functional forms for the lower cutoffs that we choose to be smooth so as to facilitate the calculation of the probability function $f_{\mathrm{on}}(t)$.

The probability function $f_{\mathrm{on}}(t)$ of a CQD can be derived from the probability density functions of on and off times for single QDs, $p_{nf(fn)}(t)$ [29],

$$f_{\mathrm{on}}(s) = \frac{\alpha + (1-\alpha)\cdot p_{fn}(s)}{1 - p_{fn}(s)\cdot p_{nf}(s)} \cdot \frac{1 - p_{nf}(s)}{s}, \tag{1}$$

where α is the proportion of QDs that are initially "on" at time $t=0$. α is effectively the initial quantum yield of the sample, assuming that a dot that is "on" has a quantum yield of unity. $p_{nf(fn)}(t)dt$ follow the relationship $p_{nf(fn)}(t)=dP_{\mathrm{on(off)}}(t)/dt$, where $1-P_{\mathrm{on(off)}}(t)$ are the cumulative distribution functions for on(off) times [i.e., the probability that a QD still remains "on" ("off") a time t after the last switching event] as expressed in Eq. (2),

$$1 - P_{\mathrm{on(off)}}(t) = (1 + t/t^{\mathrm{min}}_{\mathrm{on(off)}})^{-\mu_{\mathrm{on(off)}}} \cdot \exp(-t/t^{\mathrm{max}}_{\mathrm{on(off)}}), \tag{2}$$

where $t^{\mathrm{max}}_{\mathrm{on(off)}}$ and $t^{\mathrm{min}}_{\mathrm{on(off)}}$ are effective upper and lower cut-offs for the on(off)-time power laws, and $\mu_{\mathrm{on(off)}}$ are the power-law exponents for on and off times.[29] With the smooth lower cutoffs in Eq. (2), the Laplace transforms of $P_{\mathrm{on(off)}}(t)$ are expressed in terms of incomplete gamma functions, and the expression for $f_{\mathrm{on}}(t)$ can be numerically computed. It is likely that the arbitrary functional form in Eq. (2) for the lower cutoffs deviates from the unobservable real ones. However, as is discussed later, the shape of the cutoffs does not affect the long-time dynamics, as long as the time separation between the nonuniversal short-time dynamics characterized by $t^{\mathrm{min}}_{\mathrm{on(off)}}$, and the onset of the long-time dynamics, characterized by $t^{\mathrm{max}}_{\mathrm{on}}$, is sufficiently large. For $t^{\mathrm{max}}_{\mathrm{on}}$, $t^{\mathrm{min}}_{\mathrm{on(off)}}$, the waiting time distributions expressed in Eq. (2) approximate to

$$p_{nf(fn)}(t) \approx \mu_{\mathrm{on(off)}}(t^{\mathrm{min}}_{\mathrm{on(off)}})^{-\mu_{\mathrm{on(off)}}} t^{-(1+\mu_{\mathrm{on(off)}})} \exp(-t/t^{\mathrm{max}}_{\mathrm{on(off)}}) \tag{3}$$

when $t \gg t^{\mathrm{min}}_{\mathrm{on(off)}}$. This asymptotic functional form plays a key role in later discussions.

Once the mathematical forms for $p_{fn}(s)$ and $p_{nf}(s)$ are determined from single QD statistics, the seven parameters that describe $f_{\mathrm{on}}(t)$ are α, $t^{\mathrm{min}}_{\mathrm{on}}$, $t^{\mathrm{min}}_{\mathrm{off}}$, $t^{\mathrm{max}}_{\mathrm{on}}$, $t^{\mathrm{max}}_{\mathrm{off}}$, μ_{on}, and μ_{off}. The power-law exponents μ_{on} and μ_{off} can be obtained from single QD time traces [18]. With the method described in our previous work [29], the parameters $\mu_{\mathrm{(on)off}}$, $t^{\mathrm{max}}_{\mathrm{on}}$, and $t^{\mathrm{max}}_{\mathrm{off}}$ can also be obtained from the long time fluorescence time traces of CQDs [29]. However, the parameters $t^{\mathrm{min}}_{\mathrm{on}}$, $t^{\mathrm{min}}_{\mathrm{off}}$, and α cannot be obtained directly from the fluorescence time trace of a CQD when the experimental bin size t_b is much larger than $t^{\mathrm{min}}_{\mathrm{on}}$ and $t^{\mathrm{min}}_{\mathrm{off}}$.

In our previous work, we limited our description of $f_{\mathrm{on}}(t)$ to the long-time dynamics, where we extracted experimental values for $t^{\mathrm{max}}_{\mathrm{on}}$ and $t^{\mathrm{max}}_{\mathrm{off}}$. In this paper, we now describe how $t^{\mathrm{min}}_{\mathrm{on}}$, $t^{\mathrm{min}}_{\mathrm{off}}$, and α, and the extent of time separation affect both the short and long time behavior of $f_{\mathrm{on}}(t)$. We fix the upper cutoffs and the power law exponents as follows: $t^{\mathrm{max}}_{\mathrm{on}}=10^2$ s, $t^{\mathrm{max}}_{\mathrm{off}}=10^3$ s, and $\mu_{\mathrm{on}}=\mu_{\mathrm{off}}=0.5$. The upper cutoff values are arbitrarily chosen and lie within the experimentally observed range. The power law exponents are also consistent with experiments. Section III examines how varying $t^{\mathrm{max}}_{\mathrm{on}}/t^{\mathrm{min}}_{\mathrm{on(off)}}$, which characterizes the time separation between short and long time dynamics, affects $f_{\mathrm{on}}(t)$. Section III also derives equations for the values of the transient equilibrium and steady states that only depend on the ratios $t^{\mathrm{min}}_{\mathrm{off}}/t^{\mathrm{min}}_{\mathrm{on}}$ and $t^{\mathrm{max}}_{\mathrm{off}}/t^{\mathrm{max}}_{\mathrm{on}}$ in the limit of large time separation. We empirically

further examine the effect of time separation on $f_{on}(t)$ in Sec. IV. Sections V, VII, and IX discuss the cases where $t_{on}^{min} \cong t_{off}^{min}$, $t_{on}^{min} < t_{off}^{min}$, and $t_{on}^{min} > t_{off}^{min}$, respectively, with varying α values. Sections VI and VIII discuss experimental examples for each case and introduce a methodology to extract amplitudes of the transient equilibrium and the steady states from experiment.

III. THEORETICAL EXPLORATION OF THE EFFECT OF TIME SEPARATION BETWEEN SHORT- AND LONG-TIME DYNAMIC REGIMES ON $f_{on}(t)$

In this section, we explore the effect of time separation between short- and long-time dynamic regimes on the transient equilibrium and steady state values of $f_{on}(t)$. We use $t_{on}^{max}/t_{on(off)}^{min}$ to characterize the time separation between the larger of the lower cutoffs and the on-time upper cutoff. To understand the effect of $t_{on}^{max}/t_{on(off)}^{min}$ on the transient equilibrium state and the long-time dynamics, it is useful to divide time into three windows (1) $t_{on(off)}^{min} \ll t < t_{on}^{max}$, (2) $t_{on}^{max} < t < t_{off}^{max}$, and (3) $t_{off}^{max} < t$. In the first time window, according to Eq. (3), both probability density functions for on and off times are approximated as power laws $p_{fn}(t) \sim \varepsilon_{fn} t^{-(1+\mu_{off})}$ and $p_{nf}(t) \sim \varepsilon_{nf} t^{-(1+\mu_{on})}$, where $\varepsilon_{nf(fn)} = \mu_{on(off)} (t_{on(off)}^{min})^{\mu_{on(off)}}$. In this time window, the small-s expansion of the Laplace transforms can be approximated as $p_{fn}(s) \approx 1 + \Gamma(-\mu_{off}) \varepsilon_{fn} s^{\mu_{off}}$ and $p_{nf}(s) \approx 1 + \Gamma(-\mu_{on}) \varepsilon_{nf} s^{\mu_{on}}$. These forms create a transient equilibrium state $f_{on}^{\ te}$ for $f_{on}(t)$, when $\mu_{on} = \mu_{off} = \mu$, which is

$$f_{on}^{\ te} \approx \frac{\varepsilon_{nf}}{\varepsilon_{fn} + \varepsilon_{nf}} + \left(\frac{C_{on(off)}}{t} \right)^{1-\mu}, \tag{4a}$$

$$f_{on}^{\ te} \overset{t_{on}^{max}/t_{on(off)}^{min} \gg 1}{\approx} \frac{(t_{on}^{min})^{\mu}}{(t_{off}^{min})^{\mu} + (t_{on}^{min})^{\mu}} = \frac{1}{1 + (t_{off}^{min})^{\mu}/(t_{on}^{min})^{\mu}}, \tag{4b}$$

where $C_{on(off)}$ are correction factors specific to the mathematical forms of the on- and off-waiting time distributions. The constant $C_{on(off)}$ is on the order of $t_{on(off)}^{min}$ for the mathematical forms described in Eq. (3) so that the second term in Eq. (4a) can be neglected when $t_{on}^{max}/t_{on(off)}^{min} \gg 1$. As a result, $f_{on}^{\ te}$ becomes only a function of $t_{off}^{min}/t_{on}^{min}$ and μ as demonstrated in Eq. (4b). This suggests that, although the specific mathematical forms for the lower cutoffs are not known, they do not affect the expression for $f_{on}^{\ te}$ as long as $t_{on}^{max}/t_{on(off)}^{min} \gg 1$.

We now briefly discuss the behavior of $f_{on}(t)$ in the first time window when $\mu_{on} \neq \mu_{off}$. If $\mu_{on} > \mu_{off}$, $f_{on}(t)$ decays as a power law in the first time window with exponent $\mu_{on} - \mu_{off}$ [35,36], $f_{on}(t) \propto t^{-(\mu_{on}-\mu_{off})}$ $(t_{on(off)}^{min} \ll t < t_{on}^{max})$, which allows determination of the difference in exponents. Similarly, if $\mu_{on} < \mu_{off}$, $f_{on}(t)$ increases in the first time window as $1 - f_{on}(t) \propto t^{-(\mu_{off}-\mu_{on})}$.

In the second time window $(t_{on}^{max} < t < t_{off}^{max})$, the on-time upper cutoff becomes apparent but the off-time still behaves as a power law. As a result, $f_{on}(t)$ decays as a power law, $f_{on}(t) \propto t^{-(1-\mu_{off})}$, which allows estimation of the on-time upper cutoff, t_{on}^{max}, roughly at the onset of the power-law decay, and of the off-time power-law exponent μ_{off}. If $\mu_{on} \neq \mu_{off}$, one can determine $\mu_{on} - \mu_{off}$ in the first time window as previously explained, therefore both power-law exponents can be determined by observing the behavior of $f_{on}(t)$ in the first two windows.

In the third time window $(t_{off}^{max} < t)$, the cutoffs of both waiting-time distributions become apparent and $f_{on}(t)$ approaches a final steady state $f_{on}^{\ SS}$. The steady state value is determined by the mean on and off waiting times $\langle t_{on} \rangle$ and $\langle t_{off} \rangle$, resulting in $f_{on}^{\ SS} \approx \langle t_{on} \rangle / (\langle t_{on} \rangle + \langle t_{off} \rangle) = 1/(1 + \langle t_{off} \rangle / \langle t_{on} \rangle)$. The transition point where the trace deviates from the power-law decay can be approximated as the off-time upper cutoff t_{off}^{max} [29]. The mean on- and off-time values can, in principle, be calculated directly from the probability density functions as presented in Eq. (2), where we assumed arbitrary functional forms for the lower cutoffs. Although the lower cutoff functional forms are not obtained from experiments, the mean values are insensitive to the forms in the limit $t_{on}^{max}/t_{on(off)}^{min} \gg 1$. To demonstrate this point, we fix identical functional forms for the lower cutoffs so that $\varepsilon_{nf(fn)} \approx \mu_{on(off)} (t_{on(off)}^{min})^{\mu_{on(off)}}$, and we use exponential upper cutoffs, so the waiting-time distributions have the forms $p_{fn}(t)$ $\varepsilon_{fn} t^{-(1+\mu_{off})} e^{-t/t_{off}^{max}}$ and $p_{nf}(t)$ $\varepsilon_{nf} t^{-(1+\mu_{on})} e^{-t/t_{on}^{max}}$ [see Eq. (3)]. In the Laplace domain, these distributions can be approximated for small s as $p_{fn}(s) \approx 1 - \Gamma(-\mu_{off}) \varepsilon_{fn} (s + 1/t_{off}^{max})^{\mu_{off}} - C'_{off} s$ and $p_{nf}(s) \approx 1 - \Gamma(-\mu_{on}) \varepsilon_{nf} (s + 1/t_{on}^{max})^{\mu_{on}} - C'_{on} s$, where $C'_{on(off)}$ are correction factors, on the order of $t_{on(off)}^{min}$. The mean values for on and off times become $\langle t_{on(off)} \rangle = C'_{on(off)} - \mu_{on(off)} \Gamma(-\mu_{on(off)}) \varepsilon_{nf(fn)} (t_{on(off)}^{max})^{1-\mu_{on(off)}}$. If $\varepsilon_{nf(fn)} (t_{on(off)}^{max})^{1-\mu_{on(off)}}$ is large relative to $C'_{on(off)}$ (implying $t_{on}^{max}/t_{on(off)}^{min} \gg 1$), one can approximate the steady state value, as

$$f_{on}^{\ SS} \approx \frac{1}{1 + \{[\mu_{off} \Gamma(-\mu_{off}) \varepsilon_{fn}]/[\mu_{on} \Gamma(-\mu_{on}) \varepsilon_{nf}]\} [(t_{off}^{max})^{1-\mu_{off}}/(t_{on}^{max})^{1-\mu_{on}}]}. \tag{5}$$

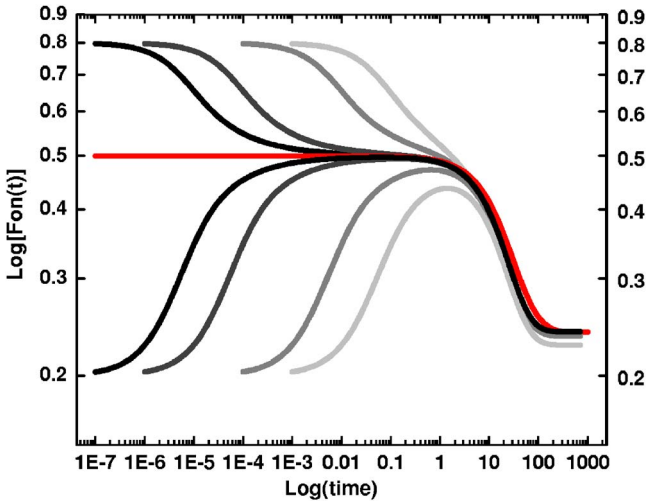

FIG. 1. (Color online) $\log_{10}$–$\log_{10}$ plots of $f_{on}(t)$ vs time with $t_{on}^{max}=10^2$ and $t_{off}^{max}=10^3$ s under different conditions. The red line (the initial flat line in gray scale) has $\alpha=0.5$ and $t_{on}^{min}\cong t_{off}^{min}=10^{-6}$, 10^{-4}, 10^{-2}, and 10^{-1} s (the curves overlap); the upper curves have $\alpha=0.9$ with $t_{on}^{min}\cong t_{off}^{min}=10^{-6}$, 10^{-4}, 10^{-2}, and 10^{-1} s from left to right; the lower curves have $\alpha=0.1$ with $t_{on}^{min}\cong t_{off}^{min}=10^{-6}$, 10^{-4}, 10^{-2}, and 10^{-1} s from left to right.

The key point of Eq. (5) is as follows: if $\mu_{on}=\mu_{off}=\mu$, as used in our current model, the steady state value only depends on the ratios $t_{off}^{max}/t_{on}^{max}$ and $t_{off}^{min}/t_{on}^{min}$ [since $\varepsilon_{fn}/\varepsilon_{nf}=(t_{off}^{min}/t_{on}^{min})^{\mu}$].

It is worth noting that Eq. (5) is still consistent with calculations using sharp cutoffs and with $\mu_{on}=\mu_{off}=0.5$. As for the waiting time distributions considered above, $\varepsilon_{nf(fn)}$ with sharp cutoffs is approximately proportional to $(t_{on}^{min}/t_{off}^{min})^{0.5}$. This results in the simple expressions $f_{on}{}^{te}=1/[1+(t_{off}^{min}/t_{on}^{min})^{0.5}]$ and $f_{on}{}^{SS}=1/[1+(t_{off}^{min}/t_{on}^{min})^{0.5}\cdot(t_{off}^{max}/t_{on}^{max})^{0.5}]$.

The errors in the values of $f_{on}{}^{te}$ and $f_{on}{}^{SS}$ that result from using Eqs. (4b) and (5) depend on the extent to which $t_{on}^{max}/t_{on(off)}^{min}>1$. With insufficient time separation, the exact expressions for $f_{on}{}^{te}$ and $f_{on}{}^{SS}$ depend on the mathematical forms for the lower cutoffs and, in principle, $f_{on}{}^{te}$ and $f_{on}{}^{SS}$ should be solved numerically. However, the following examples suggest that, in practice, these errors are small, so that Eqs. (4b) and (5) can still be applied even when the time separation appears inadequate.

IV. EMPIRICAL EXPLORATION OF THE EFFECT OF TIME SEPARATION BETWEEN SHORT- AND LONG-TIME DYNAMIC REGIMES

In this section, we empirically explore the effect of the time separation between short and long time dynamics in terms of the ratio $t_{on}^{max}/t_{on(off)}^{min}$. We focus on the formation of the transient equilibrium state and the amplitudes $f_{on}{}^{te}$ and $f_{on}{}^{SS}$. Figure 1 shows numerically generated traces for $f_{on}(t)$ using Eqs. (1) and (2). The ratio $t_{on}^{max}/t_{on(off)}^{min}$ is set at 10^8, 10^6, 10^4, and 10^3 while α is fixed at 0.9 (upper curves), 0.5 [red curve (initial flat line in gray-scale print)], and 0.1 (lower curves). A few observations are notable. (1) The shape of $f_{on}(t)$ is insensitive to the ratio $t_{on}^{max}/t_{on(off)}^{min}$ for $\alpha=0.5$. (2) For the gray ($t_{on}^{max}/t_{on(off)}^{min}=10^4$) and light gray ($10^3$) curves that transient equilibrium states are not well defined and their steady state values are lower than those of the black (10^8) and dark gray (10^6) curves. This indicates that when $t_{on}^{max}/t_{on(off)}^{min}$ is roughly less than 10^4, the short- and long-time dynamics are no longer well separated. Table I summarizes values for $f_{on}{}^{te}$, $f_{on}{}^{SS}$, and $f_{on}{}^{te}/f_{on}{}^{SS}$ for different $t_{on}^{max}/t_{on(off)}^{min}$, extracted from Fig. 1. We choose $f_{on}{}^{te}$ to be where $df_{on}(t)/dt=0$ for the gray and light gray curves whose transient equilibrium states are not well defined.

TABLE I. Values for $f_{on}{}^{te}$, $f_{on}{}^{SS}$, and $f_{on}{}^{te}/f_{on}{}^{SS}$ calculated from different $t_{on}^{max}/t_{on(off)}^{min}$ values that are used to create the plots in Fig. 1.

$t_{on}^{max}/t_{on(off)}^{min}$	$f_{on}{}^{te}$	$f_{on}{}^{SS}$	$f_{on}{}^{te}/f_{on}{}^{SS}$
10^8	0.500	0.239	2.092
10^6	0.500	0.239	2.092
10^4	0.471	0.235	2.004
10^3	0.437	0.226	1.934

Surprisingly, the values for $f_{on}{}^{te}$, $f_{on}{}^{SS}$, and $f_{on}{}^{te}/f_{on}{}^{SS}$, when $t_{on}^{max}/t_{on(off)}^{min}<10^4$, are approximately the same as those when $t_{on}^{max}/t_{on(off)}^{min}>10^4$. This implies that we can still use Eqs. (4b) and (5) to extract $t_{on}^{max}/t_{on(off)}^{min}$, $f_{on}{}^{te}$, and $f_{on}{}^{SS}$, even when $t_{on}^{max}/t_{on(off)}^{min}<10^4$.

V. THEORETICAL $f_{on}(t)$ WITH $t_{on}^{min}\cong t_{off}^{min}$

We investigate the behavior of $f_{on}(t)$ for the case of symmetric lower cutoffs for on and off times, as was the case assumed in our previous work [29]. Traces for $f_{on}(t)$ in Fig. 2 are constructed following the method detailed in the background section with $\mu_{on(off)}=\mu=0.5$, $t_{on(off)}^{min}=10^{-4}$ s, $t_{on}^{max}=10^2$, $t_{off}^{max}=10^3$ s, and $\alpha=0.1$ (green), 0.5 (black), and 0.9 (red). The traces are approximately constant at $f_{on}(t)=\alpha$ from 10^{-8}–10^{-6} s. When t approaches $t_{on}^{min}=10^{-4}$ s, $f_{on}(t)$ decays (when $\alpha=0.9$) or rises (when $\alpha=0.1$) to a transient equilibrium state value. The shape of the gradual rise or decay depends on the mathematical forms that were chosen for smooth lower cutoffs. In Fig. 2, the on- and off-time upper cutoffs t_{on}^{max} and t_{off}^{max}, are observed roughly at the transitions from the transient equilibrium state to the approximate power-law decay, and from the decay to the steady state, as indicated by the arrows at 10^2 and 10^3 s, respectively [29]. The transient equilibrium state occurs for the three time traces with $f_{on}{}^{te}=0.500$, and the steady state appears with $f_{on}^{SS}=0.239$. We show below that these values are in agreement with the values calculated using the methodology developed below in Sec. VI.

It is clear from Fig. 2 that the three time traces exhibit common long-time dynamics following a transient equilibrium state, consisting of (1) an approximate power-law decay with an exponent of $1-\mu$ and (2) an eventual steady state.

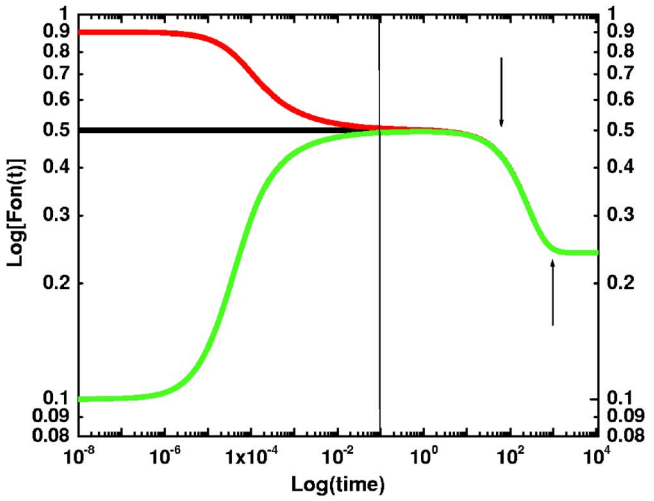

FIG. 2. (Color online) $\log_{10}$–$\log_{10}$ plots of $f_{on}(t)$ vs time with $t_{on}^{min} \cong t_{off}^{min} = 10^{-4}$ s, $t_{on}^{max} = 10^{2}$, $t_{off}^{max} = 10^{3}$ s, and with $\alpha = 0.1$ (green), 0.5 (black), and 0.9 (red) [in gray scale, $\alpha = 0.1$ (light gray), 0.5 (black), and 0.9 (gray)]. The intrinsic bin-size is arbitrarily set at 10^{-8} s.

We show in the next section that α does affect the short-time dynamics and the transient equilibrium state when the time separation between the lower cutoffs, $t_{on(off)}^{min}$, and the on-time upper cutoff t_{on}^{max} is not large enough. The short-time dynamics, which appear before the transient equilibrium state, depend on α and the functional forms for the lower cutoffs. Experimentally these non-universal short-time dynamics are largely hidden because the typical bin size (0.1 to ~ 1 s) averages over them. With a typical bin size, all three time traces in Fig. 1 would map onto the same effective time trace.

VI. EXPERIMENTAL $f_{on}(t)$ WITH $t_{on}^{min} \cong t_{off}^{min}$

We have thus far explored $f_{on}(t)$ for a CQDs theoretically. In experiments, the detector resolution is generally a few orders of magnitude larger than the lower cut-offs so that the short-time dynamics can be hidden within the first bin. The consequences of these dynamics are however reflected in the absolute values of the transient equilibrium and steady states. To properly extract these absolute values from experiments, the full behavior of $f_{on}(t)$ must be considered. This is important because $f_{on}(t)$ represents an effective QY time trace for a CQD.

The procedure to extract $t_{off}^{min}/t_{on}^{min}$, $f_{on}{}^{te}$, and $f_{on}{}^{SS}$ from an experimental fluorescence intensity trace using Eqs. (4b) and (5) is described as follows: (1) The ratios $t_{off}^{max}/t_{on}^{max}$ and $f_{on}{}^{te}/f_{on}{}^{SS}$ can be obtained directly from the experimental trace, (2) the ratio of Eqs. (4b) and (5) is then used to obtain $t_{off}^{min}/t_{on}^{min}$, (3) then the values for $t_{off}^{min}/t_{on}^{min}$ and $t_{off}^{max}/t_{on}^{max}$ are used in Eqs. (4b) and (5) to obtain absolute values for $f_{on}{}^{te}$ and $f_{on}{}^{SS}$, respectively. We demonstrate this procedure in the following examples.

Figure 3 is the fluorescence intensity time trace of a collection of CdSe QDs, synthesized as in the Ref. [37]. t_{on}^{max} and t_{off}^{max} are observed at 34 and 1570 s, respectively, so that $t_{off}^{max}/t_{on}^{max} = 47$. In addition, the ratio between the measured values of the transient equilibrium state and the steady state is ~ 4.0. Using the procedure above, these two ratios result in $f_{on}{}^{SS} = 0.125$, $f_{on}{}^{te} = 0.50$, and $t_{off}^{min}/t_{on}^{min} \sim 1$. The trace in Fig. 3 has an initial small brightening, suggesting that $\alpha < 0.5$ (as in the green curve in Fig. 1). Our analysis suggests that this sample has a QY that is initially <0.5 and that its QY rises to 0.5 before decaying to 0.125. We have found symmetric lower cutoffs often from bare CdSe and far less often from CdSe(ZnS) QDs spin-coated on bare glass substrates or in polymer matrices.

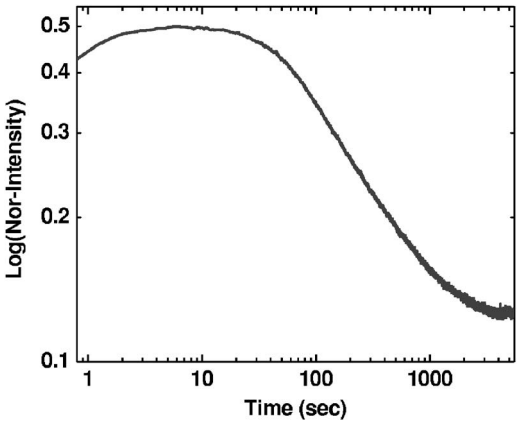

FIG. 3. $\log_{10}$–$\log_{10}$ plot of the fluorescence time trace of a collection of bare CdSe QDs excited at 514 nm with an excitation intensity flux of 15 kW/cm^2. The first absorption peak of the QD/hexane solution was at 592 nm and the diluted solution was spin coated on a bare glass substrate.

VII. THEORETICAL $f_{on}(t)$ WITH $t_{on}^{min} < t_{off}^{min}$

The next case explored is when $t_{off}^{min}/t_{on}^{min} = 10^{2}$. We set $t_{on}^{min} = 10^{-4}$ s, $t_{off}^{min} = 10^{-2}$ s, $t_{on}^{max} = 10^{2}$ s, and $t_{off}^{max} = 10^{3}$ s with $\alpha = 0.1$, 0.5, and 0.9. In Fig. 4, the steady state value appears at $f_{on}{}^{SS} = 0.030$ and the transient equilibrium state value appears at $f_{on}{}^{te} = 0.090$, which correspond to the values calculated from Eqs. (4b) and (5). In this figure, the three curves share the same long-time dynamics while the short-time dynamics exhibit non-universal features that are a consequence of asymmetric lower cutoffs and that depend on the value of α. The values of $f_{on}{}^{SS}$ and $f_{on}{}^{te}$ are lower than the corresponding values seen in Fig. 2 because $t_{on}^{min} < t_{off}^{min}$. We describe a methodology to extract model parameters from experimental traces in the next section.

VIII. EXPERIMENTAL $f_{on}(t)$ WITH $t_{on}^{min} < t_{off}^{min}$

The experimental trace shown in Fig. 5 is clearly a case with insufficient time separation. A large brightening appears at early times, and the transient equilibrium state is not quite well formed, which suggests that α is smaller than $f_{on}{}^{te}$, and the time separation between the lower and upper cutoffs is not large. However, we can still assume that the time separation is large enough to allow us to quantify this time trace as we have empirically validated in the previous section. We

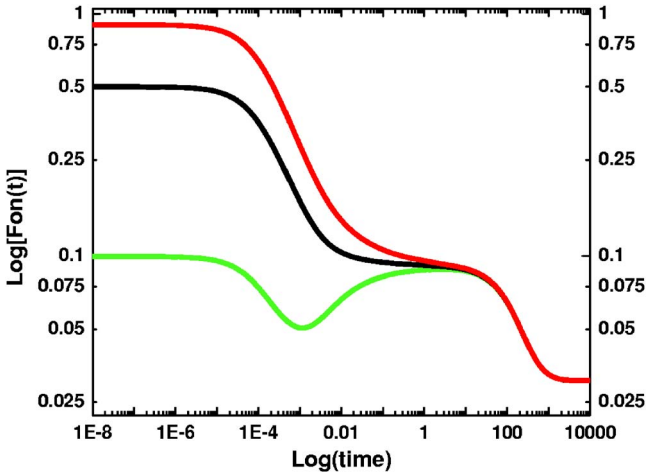

FIG. 4. (Color online) $\log_{10}$–$\log_{10}$ plots of $f_{on}(t)$ vs time with $t_{on}^{min}=10^{-4}$ s, $t_{off}^{min}=10^{-2}$ s, $t_{on}^{max}=10^{2}$, and $t_{off}^{max}=10^{3}$ s, and with $\alpha=0.1$ (green), 0.5 (black), and 0.9 (red) [in gray scale, $\alpha=0.1$ (light gray), 0.5 (black), and 0.9 (gray)]. The intrinsic bin-size is arbitrarily set at 10^{-8} s.

find $t_{on}^{max}=27$ s and $t_{off}^{max}=540$ s from the time trace so that the ratio is $t_{off}^{max}/t_{on}^{max}\cong 20$. We choose $f_{on}{}^{te}$ to be the maximum value of the trace after the initial brightening. We experimentally obtain $f_{on}{}^{te}/f_{on}{}^{SS}=5.500$, from which we estimate $t_{off}^{min}/t_{on}^{min}\cong 2.4$ using Eqs. (4b) and (5). Combining this with the experimental ratio for $t_{off}^{max}/t_{on}^{max}$, the transient equilibrium state and the steady state are calculated from Eqs. (4b) and (5) as $f_{on}{}^{te}=0.303$ and $f_{on}{}^{SS}=0.085$. The QY of this CQD in the long-time limit decreases from ~0.3 to 0.085%, which are lower than those of the first example in Sec. VI. The case $t_{on}^{min}<t_{off}^{min}$ is the one most frequently observed experimentally.

IX. THEORETICAL $f_{on}(t)$ WITH $t_{on}^{min}>t_{off}^{min}$

The last case modeled is $t_{on}^{min}=10^{-2}$ s, $t_{off}^{min}=10^{-4}$ s, $t_{on}^{max}=10$ s, and $t_{off}^{max}=10^{2}$ s with $\alpha=0.1$, 0.5, and 0.9. As shown in Fig. 6, the transient equilibrium state and the steady state values are $f_{on}{}^{te}=0.90$ and $f_{on}{}^{SS}=0.76$, far higher than the ones observed in Figs. 2 and 4, and the value of $f_{on}{}^{te}/f_{on}{}^{SS}$ is the smallest among all three cases. Overall increases in $f_{on}(t)$ are observed in the short-time window ($t<10$), from $f_{on}(t)=\alpha$ to $f_{on}{}^{te}$; the mean value for the on times in this time window is greater than the mean off time. QDs described by these parameters have higher values of $f_{on}{}^{te}$ and $f_{on}{}^{SS}$ compared to those described with the previous two cases. However, QDs with this phenomenology have not yet been observed experimentally.

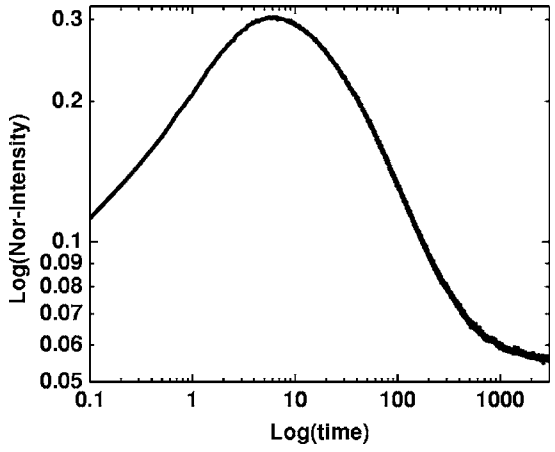

FIG. 5. $\log_{10}$–$\log_{10}$ plot of the fluorescence time trace of a collection of core(shell) CdSe(ZnS) QDs excited at 514 nm with an excitation intensity flux of 30 kW/cm^2. The first absorption peak was at 570 nm and the sample was prepared as for Fig. 3. This experimental trace gives $t_{off}^{max}=540$ s and $t_{on}^{max}=27$ s ($t_{off}^{max}/t_{on}^{max}\cong 20$). The y axis is normalized so that the peak of the curve is set at 0.303, the extracted value for $f_{on}{}^{te}$.

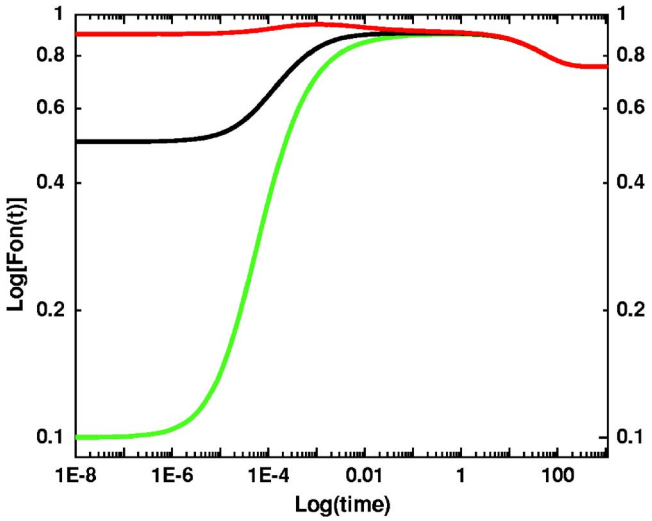

FIG. 6. (Color online) $\log_{10}$–$\log_{10}$ plots of $f_{on}(t)$ vs time with $t_{on}^{min}=10^{-4}$ s, $t_{off}^{min}=10^{-2}$ s, $t_{on}^{max}=10^{2}$, and $t_{off}^{max}=10^{3}$ s, and with $\alpha=0.1$ (green), 0.5 (black), and 0.9 (red) [in gray scale, $\alpha=0.1$ (light gray), 0.5 (black), and 0.9 (gray)]. The intrinsic bin-size is arbitrarily set at 10^{-8} s.

X. CONCLUSION

In summary, this paper explores the non-universal dynamics that appear in fluorescence time traces of CQDs at short time scales. Combined with our previous analysis for the longer time scales [10], the phenomenology of the entire fluorescence time trace of a CQD is now described purely in terms of the model parameters that characterize the blinking statistics of single QDs. Experimental observations indicate that the phenomenology of the fluorescence time trace at short times depends on the type of QD and other experimental conditions. Theoretically, we find that the diversity exhibited in the short-time dynamics is contained in the parameters α, t_{on}^{min}, and t_{off}^{min}, implying that these three model parameters distill the relevant microscopic information. We suggest a methodology to extract the model parameters from experimental data. In addition, we explore the effect of the time separation between the short- and long-time dynamics on the fluorescence time traces of CQDs. We show that the transient equilibrium state is not well defined and the values of $f_{on}{}^{te}$ and $f_{on}{}^{SS}$ both decrease when this separation is not sufficiently large, or $t_{on}^{max}/t_{on(off)}^{min}<10^{4}$, a condition which we empirically determined through simulations. We find, how-

ever, that the effect of time-scale separation on f_{on}^{te} and f_{on}^{SS} is relatively small, validating the assumption of large time separations when determining statistical parameters from experimental data.

We explore theoretical time traces for the cases $t_{on}^{min} \cong t_{off}^{min}$, $t_{on}^{min} < t_{off}^{min}$, and $t_{on}^{min} > t_{off}^{min}$. We present experimental time traces for the two cases $t_{on}^{min} \cong t_{off}^{min}$ and $t_{on}^{min} < t_{off}^{min}$ and we compare these to our model and extract model parameters. For given upper cut-offs, our theory predicts that both f_{on}^{te} and f_{on}^{SS} are highest when $t_{on}^{min} > t_{off}^{min}$, decreasing as $t_{on}^{min} \cong t_{off}^{min}$ and $t_{on}^{min} < t_{off}^{min}$.

ACKNOWLEDGMENTS

We thank Professor Robert Silbey and Dr. Vassily Lubchenko for enlightening discussions. We thank the NSF funded (Grant No. CHE-0111370) MIT Harrison Spectroscopy Laboratory for support and use of its facilities. This research was funded in part through the NSF-Materials Research Science and Engineering Center program (Grant No. DMR-0213282), by the Department of Energy (Grant No. DE-FG02-02ER45974), and by the Packard Foundation (Grant No. 2001-17717).

[1] V. I. Klimov *et al.*, Science **290**, 314 (2000).
[2] V. C. Sundar, H. J. Eisler, and M. G. Bawendi, Adv. Mater. (Weinheim, Ger.) **14**, 739 (2002).
[3] M. Kazes *et al.*, Adv. Mater. (Weinheim, Ger.) **14**, 317 (2002).
[4] A. V. Malko *et al.*, Appl. Phys. Lett. **81**, 1303 (2002).
[5] P. T. Snee *et al.*, Adv. Mater. (Weinheim, Ger.) **17**, 1131 (2005).
[6] V. L. Colvin, M. C. Schlamp, and A. P. Alivisatos, Nature (London) **370**, 354 (1994).
[7] M. C. Schlamp, X. G. Peng, and A. P. Alivisatos, J. Appl. Phys. **82**, 5837 (1997).
[8] H. Mattoussi *et al.*, J. Appl. Phys. **83**, 7965 (1998).
[9] S. Coe *et al.*, Nature (London) **420**, 800 (2002).
[10] N. Tesster *et al.*, Science **295**, 1506 (2002).
[11] M. Dahan *et al.*, Science **302**, 442 (2003).
[12] D. R. Larson *et al.*, Science **300**, 1434 (2003).
[13] D. S. Lidke *et al.*, Nat. Biotechnol. **22**, 198 (2004).
[14] J. K. Jaiswal *et al.*, Nat. Methods **1**, 73 (2004).
[15] X. Michalet *et al.*, Science **307**, 538 (2005).
[16] A. L. Efros and M. Rosen, Phys. Rev. Lett. **78**, 1110 (1997).
[17] W. E. Moerner, Science **277**, 1059 (1997).
[18] M. Kuno *et al.*, J. Chem. Phys. **112**, 3117 (2000).
[19] M. Kuno *et al.*, Phys. Rev. B **67**, 125304 (2003).
[20] K. T. Shimizu *et al.*, Phys. Rev. B **63**, 205316 (2001).
[21] M. Nirmal *et al.*, Nature (London) **383**, 802 (1996).
[22] Y. Jung, E. Barkai, and R. J. Silbey, Chem. Phys. **284**, 181 (2002).
[23] E. Barkai and G. Margolin, Isr. J. Chem. **44**, 353 (2004).
[24] R. Metzler and J. Klafter, J. Phys. A **37**, R161 (2004).
[25] O. Malcai *et al.*, Phys. Rev. E **56**, 2817 (1997).
[26] A. Ott *et al.*, Phys. Rev. Lett. **65**, 2201 (1990).
[27] M. Pelton, D. G. Grier, and P. Guyot-Sionnest, Appl. Phys. Lett. **85**, 819 (2004).
[28] S. Hohng and T. Ha, J. Am. Chem. Soc. **126**, 1324 (2004).
[29] I. Chung and M. G. Bawendi, Phys. Rev. B **70**, 165304 (2004).
[30] H. Asami, I. Kamiya, and M. Hara, Int. J. Nanosci. **1**, 641 (2002).
[31] B. C. Hess *et al.*, Phys. Rev. Lett. **86**, 3132 (2001).
[32] V. I. Klimov *et al.*, Science **287**, 1011 (2000).
[33] L.-W. Wang *et al.*, Phys. Rev. Lett. **91**, 056404 (2003).
[34] Assuming an Auger rate of $(0.1\ \text{ns})^{-1}$ and a radiative rate of $(20\ \text{ns})^{-1}$.
[35] X. Brokmann *et al.*, Phys. Rev. Lett. **90**, 120601 (2003).
[36] R. Verberk *et al.*, Physica E (Amsterdam) **26**, 19 (2005).
[37] B. R. Fisher *et al.*, J. Phys. Chem. B **108**, 143 (2004).